UCLouvain
Institute of Mechanics,
Materials and Civil Engineering

Robust optimisation of the pathway towards a sustainable whole-energy system

A hierarchical multi-objective reinforcement-learning based approach

Doctoral dissertation presented by
Xavier RIXHON
in partial fulfillment of the requirements for
the degree of Doctor in Engineering Sciences

December 2023

Thesis committee
Pr. Francesco CONTINO (supervisor, UCLouvain)
Pr. Hervé JEANMART (supervisor, UCLouvain)
Pr. Sylvain QUOILIN (ULiège)
Dr. Stefano MORET (ETH Zurich)

Contents

Symbols

Acronyms

API	application programming interface
BECCS	bioenergy with carbon capture and storage
BEMS	building energy management system
BEV	battery electric vehicle
BTX	benzene, toluene and xylene
CAPEX	capital expenditure
CCGT	combined cycle gas turbine
CCS	carbon capture and storage
CHP	combined heat and power
CNG	compressed natural gas
DC	direct current
DHN	district heating network
DNN	deep neural network
DRL	deep reinforcement learning
ESOMs	energy system optimisation models
EnergyScope TD	EnergyScope Typical Days
EUD	end-use demand
FC	fuel cell
FEC	final energy consumed
GDP	gross domestic product
GHG	greenhouse gases
GSA	global sensitivity analysis
GWP	global warming potential
HP	heat pump
HT	high-temperature

HVC	high value chemicals
IAMs	integrated assessment models
ICE	internal combustion engine
IEA	International Energy Agency
IPCC	intergovernmental panel on climate change
IQR	interquatile range
LCA	life cycle assessment
LCOE	levelised cost of energy
LFO	light fuel oil
LOO	leave-one-out
LP	linear programming
LPG	liquefied petroleum gas
LT	low-temperature
MDP	Markov decision process
MMSA	Methanol Market Services Asia
MTBE	methyl tert-butyl ether
MTO	methanol-to-olefins
NED	non-energy demand
NG	fossil gas
NN	neural network
NRE	non-renewable energy
NSC	naphtha steam cracker
OPEX	operational expenditure
PC	principal component
PCs	principal components
PCA	Principal Component Analysis
PCE	Polynomial Chaos Expansion
PDF	probability density function
PV	photovoltaic
RE	renewable energy
RL	reinforcement learning
SAC	Soft Actor Critic
SDGs	Sustainable Development Goals
SMR	small modular reactor
SVD	singular value decomposition
TRL	technology readiness level
UQ	uncertainty quantification

VRES	variable renewable energy sources

List of publications

Limpens, G., **Rixhon, X.**, Contino, F., & Jeanmart, H. (2024). "*EnergyScope Pathway: An open-source model to optimise the energy transition pathways of a regional whole-energy system.*" In Applied Energy, (Vol. 358). URL: `https://doi.org/10.1016/j.apenergy.2023.122501`

Rixhon, X., Limpens, G., Coppitters, D., Jeanmart, H.,& Contino, F.(2022). "*The role of electrofuels under uncertainties for the Belgian energy transition.*" In Energies (Vol. 14). URL: `https://doi.org/10.3390/en14134027`

Rixhon, X., Tonelli, D., Colla, M., Verleysen, K., Limpens, G., Jeanmart, H. ,& Contino, F.(2022). "*Integration of non-energy among the end-use demands of bottom-up whole-energy system models.*" In Frontiers in Energy Research, Sec. Process and Energy Systems Engineering, (Vol. 10). URL: `https://doi.org/10.3389/fenrg.2022.904777`

Rixhon, X., Colla, M., Tonelli, D., Verleysen, K., Limpens, G., Jeanmart, H., & Contino, F.(2021). "*Comprehensive integration of the non-energy demand within a whole-energy system: Towards a defossilisation of the chemical industry in Belgium.*" In proceedings of ECOS 2021 conference (Vol. 34, p. 154).

Rixhon, X., Limpens, G., Contino, F., & Jeanmart, H. (2021). "*Taxonomy of the fuels in a whole-energy system.*" In Frontiers in Energy Research, Sec. Sustainable Energy Systems, (Vol. 9). URL: `https://doi.org/10.3389/fenrg.2021.660073`

Limpens, G., Coppitters, D., **Rixhon, X.**, Contino, F., & Jeanmart, H. (2020). "*The impact of uncertainties on the Belgian energy system: application of the Polynomial Chaos Expansion to the EnergyScope model.*" In proceedings of ECOS 2020 conference (Vol. 33, p. 711).

Chapter 1

Robustness assessment of pathway roadmaps

"The more data we have, the more likely we are to drown in it."
Nassim Nicholas Taleb, in *Fooled by Randomness: The Hidden Role of Chance in Life and in the Markets*, 2008

Assessing the robustness of a roadmap driving the transition pathway of a whole-energy system is complex, especially due to the curse of dimensionality. This curse comes from the number of variables of the system (e.g. the installed capacity of technologies), the multiple-year approach specific to the pathway optimisation (i.e. versus the snapshot approach) or the number of uncertain parameters. On top of this, the sector coupling interconnecting the installed capacities and the used resources among the different (non-)energy sectors can make harder the understanding of big trends of such a system. To navigate through this load of uncertain and interconnected data, it is necessary to assess the robustness of pathway roadmaps.

To deal with such uncertainties, decision-makers have several options: (i) resistance; (ii) resilience; (iii) static robustness; and (iv) adaptive robustness [1]. Where resistance consists in planning for the worst-case scenario, resilience aims at a fast recovery whatever the conditions in the future. Finally, in static robustness, one seeks for a roadmap that would perform "satisfactorily" in a wide range of plausible futures, whereas, a roadmap would be dynamically robust if it is prepared to adapt in case of a change in conditions. Where the adaptability of the policy was addressed in Chapter **??**, the objective of this chapter is to apply the method described in Section **??** to deal with the static robustness of pathway roadmaps. Castrejon-Campos et al. [2] assessed policy mix folllowing the same philosophy of "satisfactory level of performance" as [1]. In their work, they mostly focused on the electricity sector, accounting for a variety of stakeholders and related interests using STET (Socio-Technical Energy Transition) models to capture more properly societal and behavioral aspects in relation with policy implementation, enriching purely techno-economy model, like EnergyScope, that usually assume rational choice within an overall cost minimization. However, in the case of the transition pathway of a whole-eenrgy system, the challenges stand here in the definition of the "performance metric" as well as the "satisfactory level of performance". Between the sole total transition cost and the entire set of installed technologies that give too few and too much information, respectively, the performance metric here is defined through the Principal Component Analysis (PCA) approach. Then, when comes the "satisfactory level of performance", we propose a relative level of performance through a comparative analysis of different roadmaps. In other terms, one roadmap will not be robust or not in itself but rather more or less robust than another one.

Contributions

The main contributions of this chapter is the application of the methodology proposed in Section **??** to the case study of the Belgian energy transition. First, we develop the different steps that lead to the principal components of the transition. We analyse these big trends of variation and highlight the fact that these variations stand for the entire pathway, a group of consecutive representative years or rather on a tipping-year. Then, and most importantly, we assess the robustness of different technological roadmaps by projecting their resulting myopic pathway against these directions of variation. The application of PCA to provide a new metric for robustness applied to the case of Belgium is the added-value of this chapter.

1.1 Definition of the principal components of the transition

As detailed in Section **??**, we have decided to define the directions of variation, i.e. the robustness metrics, based on the installed capacities through the transition in the different end-use sectors, i.e. electricity, high-temperature (HT) heat, low-temperature (LT) heat, passenger mobility, freight mobility, high value chemicals (HVC), ammonia and methanol. These capacities represent the technological roadmaps to supply these end-use demand (EUD) while respecting the CO_2-budget. As introduced in Section **??**, the data considered in this method come from the global sensitivity analysis (GSA) carried out on the perfect foresight optimisation of the Belgian transition pathway (see Chapter **??**). This gave 1260 different transitions resulting, for each of them, from the pathway optimisation subject to a sample of uncertain parameters (see Section **??**). Appendix **??** gives the exhaustive distributions of the installed capacities among the different end-use sectors from the GSA.

1.1.1 Principal components of each representative year

After the pre-preprocessing of the raw data (i.e. data scaling and outliers management, see Section **??**), the principal components (PCs) of each representative year of the transition, except 2020 as the initialisation year, can be computed.

First of all, before investigating the PCs, it is worth looking at the total variance of each representative year (see Table 1.1). Even though the absolute value of these variances has no physical meaning, we observe that the variations are more important at earlier stages of the transition. In other words, the further goes the transition, the more limited are the degrees of freedom to respect the CO_2-budget.

Table 1.1. Whole-system design variance of the different representative years and their comparison with 2025.

Year	**Design variance** $[10^{-3}]$	**vs. 2025**
2025	10.4	-
2030	12.1	+15%
2035	9.7	-7%
2040	6.1	-42%
2045	5.1	-51%
2050	4.8	-54%

Then, keeping the PCs capturing at least 90% of the total variance of each representative year, this gives between four, in 2035, and seven, in 2050, PCs depending on the year (see Figure 1.1), and a total of 34 PCs. At later stages of the transition, the increasing number of required PCs, in line with their smaller share of explained variance, is another indication that the variance of the system design is more spread over a wider range of technologies and with a more limited amplitude.

Finally, we consider the respective contribution of the different technologies in the different PC_y, i.e. their corresponding component in the different eigenvectors. Highlighting the top-5 technologies for $PC_{y,1}$, $PC_{y,2}$ and $PC_{y,3}$, we observe general trends over the whole transition as well as tipping year where there is a clear trade-off between several technologies (see Figure 1.2). As pointed out in Section **??**, PCA does

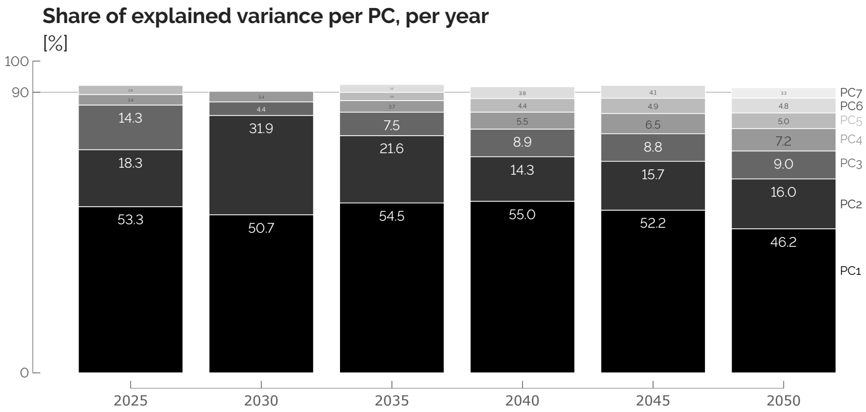

Figure 1.1. PCs capturing at least 90% of the total variance of their respective representative year of the transition.

not make any distinction between a vector of variation and its opposite. This is why $PC_{2025,1}$ and $PC_{2035,1}$ are actually very similar even though there are mostly on the opposite sides of the 0-axis.

Even though the following observations could be made by analysing the distribution of installed capacities (see Appendix **??**) or the covariance matrices, the PCA decomposition offers a more visual and summarising representation of the main trends of variation. Due to their intermittency, integrating more PV panels leads to the installation of other technologies to benefit from free and renewable electricity when it exceeds the electrical EUD. Therefore, we observe that the variation of installed PV is directly linked with the variation of installed industrial electrical resistors and, to a smaller extent, of decentralised and district heating network (DHN) electrical HP. These variations cover the whole transition as the main varying factors given their significant contributions to the PC_1. Where this was an example for correlated technologies, we can also identify some key modal shifts where one technology is either substituted by others or in balance with another one. First, about the LT heat sector, the early stages of the transition, i.e. 2025-2030, sees the shift from mainly decentralised oil and gas boilers towards decentralised and DHN electrical HP. Later in the transition, there seems to be a tight competition between (bio)diesel and fuel cell (FC) trucks that drive the design variance to a smaller extent as they mostly appear in the second and third PCs of the representative years. Not capturing a significant share of variance, there are other modal shifts (e.g. battery electric vehicle (BEV) substituting diesel and gasoline cars) that are not visible through the PCs. Besides these modal

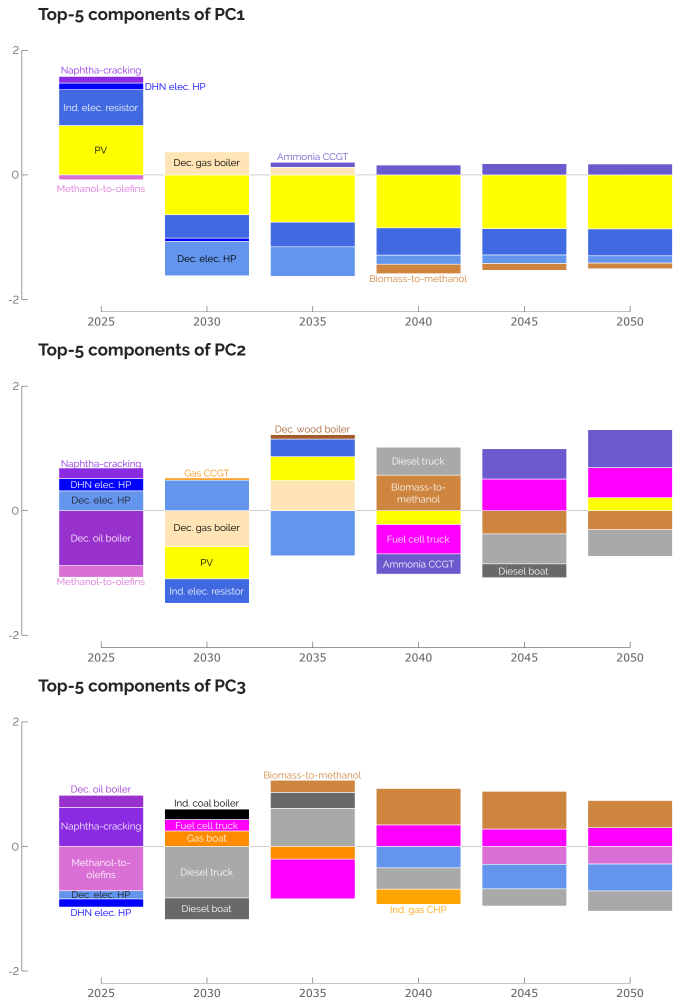

Figure 1.2. Contribution of the top-5 technologies to the first three PCs over the different representative years. Where the variation of photovoltaic (PV) panels supported by the electrification of the HT heat via industrial electric resistors is the main varying drivers over the whole transition, there are tipping years like 2025 for the production of HVC (i.e. naphtha-cracker to methanol-to-olefins (MTO) or 2025-2030 for the production of LT heat (i.e. from oil and gas boilers to electric heat pump (HP).

shifts spread over several representative years, 2025 is the tipping year concerning the shift from naphtha-cracker and methanol-to-olefins to supply HVC. Finally, there are also technologies contributing to PCs because they are the main producing assets of their respective end-use sector and the demand varies significantly, e.g. biomass-to-methanol.

1.1.2 Principal components of the transition

Based on the PCs of each representative year, PC_y, the PCs of the transition, i.e. the metrics to assess the robustness of roadmaps, can be computed. Before aggregating and averaging similar PC_y, it is necessary to rank them to ensure capturing most of the transition variance in the subsequent $PC_{transition}$.

Based on the design variance captured by each PC_y in their respective representative year, we can rank them (see Table 1.2). Summing all of these variances over the different years results in a "pseudo" total variance of the transition. To construct the PCs of the transition, $PC_{transition}$, we keep the PC_y that captures at least 80% of this total variance of the transition (see Section **??**). This results in keeping 14 PC_y: the first and second PCs of each representative year and the third PC of 2025 and 2035. Even though the 80%-threshold is reached with the first 11 PCs, $PC_{2045,2}$, $PC_{2050,2}$ and $PC_{2035,3}$ are accounted for as they are similar to $PC_{2040,2}$. Consequently, aiming at capturing at least 80% of the total transition variance,

Given the similarity between PC_y (see Figure 1.2), some $PC_{transition}$ result from the aggregation and averaging of the components of several PC_y (see Table 1.3). This aggregation step has a double objective: limiting the dimension of the robustness metrics and avoiding ineffective redundancy in terms of $PC_{transition}$ where several of them would otherwise point towards similar directions of variation.

Averaging the components of similar PC_y allows constructing the $PC_{transition}$ (see Figure 1.3). These directions of variation form the robustness matrix on which it is possible to project the results of transition roadmaps tested under uncertainties and myopic pathway optimisation.

1.2 Robustness assessment of pathway roadmaps

Now that the performance metric is defined, we can assess the robustness of different roadmaps. These roadmaps are defined as the technological mix given by the deterministic optimisation of the perfect foresight pathway under certain conditions. The two first roadmaps are the **REF** and **SMR** cases (see Chapter **??**). All the uncertain

Table 1.2. Ranking of PCs per design variance captured in their respective representative year and cumulative share of the captured total variance of the transition

Ranking	**Year**	**PC**	**Design variance** $[10^{-4}]$	**Cumulative share of total variance** [%]
1	2030	PC_1	61.1	13.9
2	2025	PC_1	55.7	26.5
3	2035	PC_1	52.7	38.4
4	2030	PC_2	38.4	47.2
5	2040	PC_1	33.4	54.7
6	2045	PC_1	26.5	60.7
7	2050	PC_1	22.2	65.8
8	2035	PC_2	20.9	70.5
9	2025	PC_2	19.1	74.8
10	2025	PC_3	15.0	78.2
11	2040	PC_2	8.7	**80.2**
12	2045	PC_2	7.9	82.0
13	2050	PC_2	7.7	83.7
14	2035	PC_3	7.3	85.4
⋮	⋮	⋮	⋮	⋮
34	2050	PC_7	1.6	100

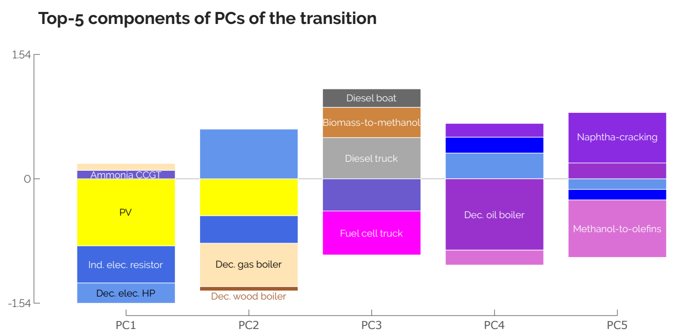

Figure 1.3. Contribution of the top-5 technologies to the different $PC_{transition}$.

Table 1.3. Aggregation of PC_y to construct the $PC_{transition}$ and share of the captured total variance of the transition by each $PC_{transition}$.

$\mathbf{PC_{transition}}$	$\mathbf{PC_y}$	**Share of total variance** [%]
$PC_{transition,1}$	$PC_{2025,1}$ $PC_{2030,1}$ $PC_{2035,1}$ $PC_{2040,1}$ $PC_{2045,1}$ $PC_{2050,1}$	57.0
$PC_{transition,2}$	$PC_{2030,2}$ $PC_{2035,2}$	13.4
$PC_{transition,3}$	$PC_{2040,2}$ $PC_{2045,2}$ $PC_{2050,2}$ $PC_{2035,3}$	7.2
$PC_{transition,3}$	$PC_{2025,2}$	4.3
$PC_{transition,4}$	$PC_{2025,3}$	3.4

parameters are considered at their nominal value in these two cases. The only difference consists in allowing small modular reactor (SMR) from 2040 onward in the **SMR** case. On top of these two cases, we add a so-called "robust" case, **ROB**, in the same sense as in the works of Bertsimas and Sim [3] or Moret [4] accounting for a "protection parameter". Then, we assess the robustness of these three roadmaps via a similar "three-step rolling horizon approach" as in the work of Moret et al. [5]: (i) setting the initial investment strategies provided by the roadmaps and, (ii) assessing the variation of investments needed through myopic pathway optimisation under uncertainties and, (iii) projecting the strategies from the myopic optimisations on the robustness metrics defined via PCA.

1.2.1 The robust roadmap

Rather than considering all the uncertain parameters at their worst values as in the work of Soyster [6], we follow here the robust approach of Bertsimas and Sim [3] and Moret [4]. In their works, the authors consider a factor $\Gamma_{obj} \in [0, d]$ that represents a "protection parameter" of the objective function where d is the total number of uncertain parameters (see Section **??**). If $\Gamma_{obj} = 0$, where all the uncertain parameters are at their nominal value, we obtain the deterministic solution of the **REF** case. If $\Gamma_{\text{obj}} = d$, this means considering the "fully robust" solution where all the uncertain parameters are their worst value, as in Soyster [6]. Between these two extreme cases, the uncertain parameters to account for at their worst values follow the ranking given by the GSA (see Chapter **??**). In practice, $\Gamma_{\text{obj}} = 1$ means considering the cost of purchasing electrofuels at its worst value. $\Gamma_{\text{obj}} = 2$ adds the industry EUD at its worst value in the lot, and so on. In the present analysis, we consider the "robust" roadmap by setting $\Gamma_{\text{obj}} = 6$. Consequently, costs of purchasing electrofuels, fossil fuels and biofuels as well as the industry EUD, the interest rate and the variable OPEX of technologies are considered at their worst values, i.e. the upper bound of their respective range. In practice, this means that, in the ROB case, imported energy carriers, except electricity, are 179.8% more expensive, the industrial demand is, by 2050, 23.9% higher[1], the interest rate is 46.2% (i.e. 2.2% versus 1.5% in the REF case) and the variable OPEX of technologies, c_{maint}, is 35.7% higher. The following paragraphs investigate the differences in the different sectors between the ROB and the REF cases, similarly to the comparison carried out with the SMR case in Chapter **??**.

Power sector

Given the more expensive imported energy carriers, the model opts for an earlier electrification of the system and more efficiency. Consequently, the power sector is one of the most impacted ones (see Figure 1.4). At the earlier stages of the transition, the model opts for the full deployment of local variable renewable energy sources (VRES) as soon as possible and importing more electricity (i.e. +8.7 TWh, +52%) from abroad in 2025. This earlier and bigger integration of VRES is supported by the higher electrification of HT and, to a smaller extent the LT, heating sector as well as in the mobility sectors. It is mostly the industrial electric heaters that absorb the abundant and intermittent electricity produced by PV panels and wind turbines. In the mobility sectors, BEV substitutes gasoline cars from 2025 onward and electric trucks make the transition from diesel to FC trucks. On the supply side, besides the local VRES and the direct import of electricity from abroad, combined heat and power (CHP) units, mostly industrial, are favoured given their higher efficiency at the expense of ammonia-combined cycle gas turbine (CCGT). In the ROB case, by 2050, these CHP units produce 43.3 TWh, i.e. 23% of the total electricity production, versus 21.9 TWh in the REF case. These observations are in line with the work of Moret

[1] As detailed in Chapter **??**, the industrial demand encompasses the whole non-energy demand (NED) and LT heat demand, as well as the industrial share of electricity and LT heat demands.

et al. [5] focusing on the problem of overcapacity in the European power sector. The authors highlighted that the robust strategy diversified the supply sources of electricity between VRES, import of electricity and more efficient technologies like CHP and HP.

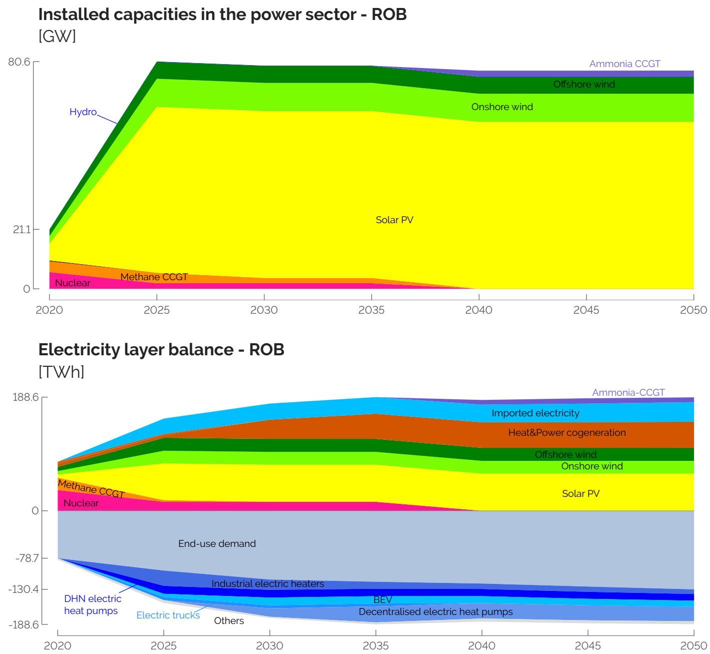

Figure 1.4. Installed capacities and layer balance of the power sector in the ROB case. Compared to the REF case, local VRES are deployed as soon as possible supported by an earlier electrification of the heat and transport sectors. CHP units also represents a higher share of the electricity supply given their higher efficiency at the expense of other flexible production units like ammonia-CCGT.

Heating sectors

By 2050, the additional 23.9% of industrial EUD directly impacts the technological mix to supply the HT heat, i.e. +13.6 TWh as direct HT heat EUD on top of the extra 3.4 TWh consumed by the MTO process. As aforementioned, at earlier stages of the transition, up to 20.9 GW of industrial electric heaters supply the additional demand and support the integration of solar PV. However, in the mid-term, 27% of these heaters are prematurely decommissioned where 24% are not renewed after reaching the end of their lifetime. Instead, up to +3.5 GW of industrial CHP units are installed to efficiently use e-methane that is considered more expensive in the ROB case to supply electricity and 52% of the HT heat demand. About the LT heat sector, the principal impact is the bigger installation of DHN and decentralised electric HP, up to +2.1 GW and +0.8 GW respectively.

Mobility sectors

In the transport of freight, the ROB roadmap transition from diesel to FC trucks with the use of electric trucks from 2025 to 2035. Similarly to the industrial electric heaters, it is a way to integrate to early installation of solar PV and absorb part of its intermittent electricity. Freight transport via trains and boats are not different from the REF roadmap. About the passenger mobility, compared to the REF case, the shift from internal combustion engine (ICE) cars to BEV occurs earlier in the transition, in line with the increased production of intermittent electricity from VRES.

Non-energy

Technologically speaking, by 2050, the ROB case accounts for an additional 1.2 GW of MTO to supply the extra 10.3 TWh of HVC. Besides this, the extra 2.5 TWh and 0.4 TWh of e-ammonia and e-methanol are supplied by supplied by the import of their respective energy carrier.

In conclusion, the two main assumptions impacting the ROB roadmap strategy compared to the REF one were the higher cost of purchasing imported energy carriers (except electricity) and higher industrial EUD.More expensive imported energy carriers lead to, on the one hand, an earlier full deployment of local VRES (i.e. PV, wind onshore and offshore) supported by a higher electrification of the heating and transport sectors. On the other hand, it increases the share of the total OPEX due to the consumption of resources (i.e. excluding the OPEX of the technologies) in the total transition cost: i.e. 56% versus 38% in the REF case. This, combined with the increase of industrial EUD, encourages a more efficient use of the resources, i.e. CHP and HP. The increased interest rate and variable OPEX of technologies have a more negligible impact on the roadmap strategy as they identically affect the entire set of technologies.

1.2.2 Projection on robustness metric

After defining the robustness metric and describing the roadmaps to assess (i.e. REF, SMR and ROB), the final step consists in testing these roadmaps under uncertainties in a myopic pathway optimisation. This aims at assessing the adaptation of the roadmaps as uncertainty gradually unfolds over time [5], which brings more realism than perfect foresight [7]. The three roadmaps are tested 500 times fixing the installed capacities $f_{\max} \geq \mathbf{F} \geq \mathbf{F}^*$ for all the end-use technologies, and taking values of the 34 uncertain parameters (see Section **??**) following the sampling technique detailed in Section **??**, i.e. Sobol' sequence. However, uncertain parameters limit the potential installed capacity, $f_{\max}$, of PV panels, onshore and offshore wind turbines and SMR. For these, in case the installed capacity prescribed by the roadmap is higher than the maximum potential affected by the value of the uncertain parameter, the actual installed capacity is set to this new limit. In reality, this would be similar to revise to a smaller extent the expected roadmap due to external events (e.g. smaller public acceptance [8, 9], lower technology readiness level (TRL) or longer installation time than expected)

1.3 Discussion

Bibliography

[1] W. E. Walker, R. J. Lempert, J. H. Kwakkel, Deep uncertainty, Delft University of Technology 1 (2012).

[2] O. Castrejon-Campos, L. Aye, F. K. P. Hui, Making policy mixes more robust: An integrative and interdisciplinary approach for clean energy transitions, Energy Research & Social Science 64 (2020) 101425.

[3] D. Bertsimas, M. Sim, The price of robustness, Operations research 52 (2004) 35–53.

[4] S. Moret, Strategic energy planning under uncertainty, Ph.D. thesis, EPFL, 2017.

[5] S. Moret, F. Babonneau, M. Bierlaire, F. Maréchal, Overcapacity in european power systems: Analysis and robust optimization approach, Applied Energy 259 (2020) 113970.

[6] A. L. Soyster, Convex programming with set-inclusive constraints and applications to inexact linear programming, Operations research 21 (1973) 1154–1157.

[7] K. Poncelet, E. Delarue, D. Six, W. D'haeseleer, Myopic optimization models for simulation of investment decisions in the electric power sector, in: 2016 13th International Conference on the European Energy Market (EEM), IEEE, 2016, pp. 1–9.

[8] J. Zoellner, P. Schweizer-Ries, C. Wemheuer, Public acceptance of renewable energies: Results from case studies in germany, Energy policy 36 (2008) 4136–4141.

[9] H. Sam-Aggrey, Small Modulator Reactors (SMRs)-the key to increased social acceptance of nuclear power?, Technical Report, Atomic Energy of Canada Limited, 2014.

[10] M. M. Dekker, V. Daioglou, R. Pietzcker, R. Rodrigues, H.-S. de Boer, F. Dalla Longa, L. Drouet, J. Emmerling, A. Fattahi, T. Fotiou, et al., Identifying energy model fingerprints in mitigation scenarios, Nature Energy 8 (2023) 1395–1404.

[11] B. S. Palmintier, Incorporating operational flexibility into electric generation planning: Impacts and methods for system design and policy analysis, Ph.D. thesis, Massachusetts Institute of Technology, 2013.

[12] D. Connolly, H. Lund, B. V. Mathiesen, M. Leahy, A review of computer tools for analysing the integration of renewable energy into various energy systems, Applied Energy 87 (2010) 1059–1082. doi:10.1016/j.apenergy.2009.09.026.

[13] P. Lopion, P. Markewitz, M. Robinius, D. Stolten, A review of current challenges and trends in energy systems modeling, Renewable and sustainable energy reviews 96 (2018) 156–166.

[14] S. Pfenninger, A. Hawkes, J. Keirstead, Energy systems modeling for twenty-first century energy challenges, Renewable and Sustainable Energy Reviews 33 (2014) 74–86.

[15] M. G. Prina, M. Lionetti, G. Manzolini, W. Sparber, D. Moser, Transition pathways optimization methodology through EnergyPLAN software for long-term energy planning, Applied Energy 235 (2019) 356–368. doi:10.1016/j.apenergy.2018.10.099.

[16] M. G. Prina, G. Manzolini, D. Moser, B. Nastasi, W. Sparber, Classification and challenges of bottom-up energy system models - a review, Renewable and Sustainable Energy Reviews 129 (2020) 109917.

[17] M. Chang, J. Z. Thellufsen, B. Zakeri, B. Pickering, S. Pfenninger, H. Lund, P. A. Østergaard, Trends in tools and approaches for modelling the energy transition, Applied Energy 290 (2021) 116731.

[18] R. Atlason, R. Unnthorsson, Ideal EROI (energy return on investment) deepens the understanding of energy systems, Energy 67 (2014) 241–245. doi:10.1016/j.energy.2014.01.096.

[19] Pfenninger and Pickering, Calliope - a multi-scale energy systems modelling framework, Accessed 2023. URL: https://www.callio.pe/.

[20] A. University, EnergyInteractive.NET, Accessed July 17th, 2018. URL: http://energyinteractive.net/.

[21] Ž. Popović, B. Brbaklić, S. Knežević, A mixed integer linear programming based approach for optimal placement of different types of automation devices in distribution networks, Electric Power Systems Research 148 (2017) 136–146.

[22] Berkeley Lab, Der-cam, Accessed June 12th, 2023. URL: https://gridintegration.lbl.gov/der-cam.

[23] A. Zerrahn, W.-P. Schill, Long-run power storage requirements for high shares of renewables: review and a new model, Renewable and Sustainable Energy Reviews 79 (2017) 1518–1534.

[24] University of Stuttgart, European Electricity Market Model, Accessed June 12th, 2023. URL: https://www.ier.uni-stuttgart.de/forschung/modelle/E2M2/.

[25] S. Backe, C. Skar, P. C. del Granado, O. Turgut, A. Tomasgard, Empire: An open-source model based on multi-horizon programming for energy transition analyses, SoftwareX 17 (2022) 100877.

[26] Quintel Intelligence, Energy Transition Model, Accessed September 17th, 2023. URL: `https://docs.energytransitionmodel.com/main/intro/`.

[27] H. Lund, J. Z. Thellufsen, Energyplan - advanced energy systems analysis computer model (version 15.1), `https://doi.org/10.5281/zenodo.4001540`, 2020. [Accessed September 17, 2020].

[28] O. Lugovoy, V. Potashnikov, energyRt: Energy systems modeling toolbox in R, development version, 2022. URL: `https://github.com/energyRt/energyRt`, r package version 0.01.21.9003.

[29] G. Limpens, S. Moret, H. Jeanmart, F. Maréchal, EnergyScope TD: A novel open-source model for regional energy systems, Applied Energy 255 (2019) 113729.

[30] Freaunhofer ISI, Enertile, Accessed June 12th, 2023. URL: `https://www.enertile.eu/enertile-en`.

[31] C. F. Heuberger, Electricity systems optimisation with capacity expansion and endogenous technology learning (eso-xel), Zenodo (2017).

[32] K. Löffler, K. Hainsch, T. Burandt, P.-Y. Oei, C. Kemfert, C. Von Hirschhausen, Designing a model for the global energy system—genesys-mod: an application of the open-source energy modeling system (osemosys), Energies 10 (2017) 1468.

[33] L. Herc, A. Pfeifer, F. Feijoo, N. Duić, Energy system transitions pathways with the new h2res model: a comparison with existing planning tool, e-Prime-Advances in Electrical Engineering, Electronics and Energy 1 (2021) 100024.

[34] R. Dufo López, ihoga, Accessed June 12th, 2023. URL: `https://ihoga.unizar.es/en/`.

[35] P. Kuhn, Iteratives Modell zur Optimierung von Speicherausbau und-betrieb in einem Stromsystem mit zunehmend fluktuierender Erzeugung, Ph.D. thesis, Technische Universität München, 2012.

[36] Electric Power Research Institute, Open distribution system simulator (opendss), Accessed June 12th, 2023. URL: `https://sourceforge.net/projects/electricdss/`.

[37] Energy Exemplar, Plexos (version 9.0), 2023. URL: `https://plexos9.com/`.

[38] V. Waucquez, Validation of the cost optimization model, pathway energyscope, for scenario analysis, 2023. URL: `http://hdl.handle.net/2078.1/thesis:40534`.

[39] T. Brown, J. Hörsch, D. Schlachtberger, Pypsa: Python for power system analysis, arXiv preprint arXiv:1707.09913 (2017).

[40] T. Brown, J. Hörsch, D. Schlachtberger, PyPSA: Python for Power System Analysis, 2018. URL: `https://pypsa.org/`.

[41] T. T. Pedersen, E. K. Gøtske, A. Dvorak, G. B. Andresen, M. Victoria, Long-term implications of reduced gas imports on the decarbonization of the european energy system, Joule 6 (2022) 1566–1580.

[42] Energistyrelsen, Modeldokumentation – Ramses energisystemmodel , Technical Report, 2023. URL: `https://ens.dk/sites/ens.dk/files/Analyser/ramses_energisystemmodel.pdf`.

[43] W. Short, P. Sullivan, T. Mai, M. Mowers, C. Uriarte, N. Blair, D. Heimiller, A. Martinez, Regional energy deployment system (ReEDS), Technical Report, National Renewable Energy Lab.(NREL), Golden, CO (United States), 2011.

[44] R. Loulou, U. Remme, A. Kanudia, A. Lehtila, G. Goldstein, Documentation for the times model part ii, Energy technology systems analysis programme (2005).

[45] IEA-ETSAP, Times model description, 2021. URL: `https://wiki.openmod-initiative.org/wiki/TIMES`.

[46] S. Pfenninger, J. Keirstead, Renewables, nuclear, or fossil fuels? Scenarios for Great Britain's power system considering costs, emissions and energy security, Applied Energy 152 (2015) 83–93. doi:`10.1016/j.apenergy.2015.04.102`.

[47] B. Pickering, R. Choudhary, Quantifying resilience in energy systems with out-of-sample testing, Applied Energy 285 (2021) 116465.

[48] S. Pfenninger, Dealing with multiple decades of hourly wind and pv time series in energy models: A comparison of methods to reduce time resolution and the planning implications of inter-annual variability, Applied energy 197 (2017) 1–13.

[49] H.-K. Bartholdsen, A. Eidens, K. Löffler, F. Seehaus, F. Wejda, T. Burandt, P.-Y. Oei, C. Kemfert, C. v. Hirschhausen, Pathways for Germany's low-carbon energy transformation towards 2050, Energies 12 (2019) 2988.

[50] M. Welsch, P. Deane, M. Howells, B. Ó. Gallachóir, F. Rogan, M. Bazilian, H.-H. Rogner, Incorporating flexibility requirements into long-term energy system models–A case study on high levels of renewable electricity penetration in Ireland, Applied Energy 135 (2014) 600–615.

[51] G. Haydt, V. Leal, A. Pina, C. A. Silva, The relevance of the energy resource dynamics in the mid/long-term energy planning models, Renewable energy 36 (2011) 3068–3074.

[52] G. Limpens, X. Rixhon, F. Contino, H. Jeanmart, Energyscope pathway: an open-source model to optimise the energy transition pathways of a regional whole-energy system, Elsevier in Applied Energy 358 (2024). doi:https://doi.org/10.1016/j.apenergy.2023.122501.

[53] G. Limpens, Pathway extension of model EnergyScope TD, Accessed 2023. URL: https://github.com/energyscope/EnergyScope_pathway/tree/v1.1.

[54] G. Limpens, EnergyScope Pathway documentation, Accessed 2022. URL: https://energyscope-pathway.readthedocs.io/en/v1.1/.

[55] V. Codina Gironès, S. Moret, F. Maréchal, D. Favrat, Strategic energy planning for large-scale energy systems: A modelling framework to aid decision-making, Energy 90, Part 1 (2015) 173–186. doi:10.1016/j.energy.2015.06.008.

[56] F. Y. Kuo, I. H. Sloan, Lifting the curse of dimensionality, Notices of the AMS 52 (2005) 1320–1328.

[57] P. Gabrielli, M. Gazzani, E. Martelli, M. Mazzotti, Corrigendum to "Optimal design of multi-energy systems with seasonal storage" [Appl. Energy (2017)], Applied Energy 212 (2018) 720. doi:10.1016/j.apenergy.2017.12.070.

[58] J. Després, S. Mima, A. Kitous, P. Criqui, N. Hadjsaid, I. Noirot, Storage as a flexibility option in power systems with high shares of variable renewable energy sources: a POLES-based analysis, Energy Economics 64 (2017) 638–650. doi:10.1016/j.eneco.2016.03.006.

[59] P. Nahmmacher, E. Schmid, L. Hirth, B. Knopf, Carpe diem: A novel approach to select representative days for long-term power system modeling, Energy 112 (2016) 430–442.

[60] J. E. Gentle, L. Kaufman, P. J. Rousseuw, Finding Groups in Data: An Introduction to Cluster Analysis., John Wiley & Sons 47 (2006) 788. doi:10.2307/2532178.

[61] H. S. Park, C. H. Jun, A simple and fast algorithm for K-medoids clustering, Expert Systems with Applications 36 (2009) 3336–3341. doi:10.1016/j.eswa.2008.01.039.

[62] F. Contino, S. Moret, G. Limpens, H. Jeanmart, Whole-energy system models: The advisors for the energy transition, Progress in Energy and Combustion Science 81 (2020) 100872. URL: https://doi.org/10.1016/j.pecs.2020.100872.

[63] X. Rixhon, G. Limpens, D. Coppitters, H. Jeanmart, F. Contino, The role of electrofuels under uncertainties for the Belgian energy transition, Energies 14 (2021) 4027.

[64] G. Limpens, S. Moret, G. Guidati, X. Li, F. Maréchal, H. Jeanmart, The role of storage in the Swiss energy transition, in: proceedings of ECOS 2019 conference, 2019, pp. 761–774.

[65] G. Limpens, H. Jeanmart, F. Maréchal, Belgian Energy Transition: What Are the Options?, Energies 13 (2020) 261.

[66] M. Borasio, S. Moret, Deep decarbonisation of regional energy systems: A novel modelling approach and its application to the italian energy transition, Renewable and Sustainable Energy Reviews 153 (2022) 111730.

[67] J. Dommisse, J.-L. Tychon, Modelling of Low Carbon Energy Systems for 26 European Countries with EnergyScopeTD : Can European Energy Systems Reach Carbon Neutrality Independently?, Master's thesis, UCLouvain, 2020. URL: http://hdl.handle.net/2078.1/thesis:25202.

[68] P. Thiran, H. Jeanmart, F. Contino, Validation of a method to select a priori the number of typical days for energy system optimisation models, Energies 16 (2023) 2772.

[69] M. Pavičević, P. Thiran, G. Limpens, F. Contino, H. Jeanmart, S. Quoilin, Bi-directional soft-linking between a whole energy system model and a power systems model, in: 2022 IEEE PES/IAS PowerAfrica, IEEE, 2022, pp. 1–5.

[70] J. Schnidrig, R. Cherkaoui, Y. Calisesi, M. Margni, F. Maréchal, On the role of energy infrastructure in the energy transition. case study of an energy independent and co2 neutral energy system for switzerland, Frontiers in Energy Research 11 (2023) 1164813. URL: https://doi.org/10.3389/fenrg.2023.1164813. doi:10.3389/fenrg.2023.1164813.

[71] G. Limpens, Generating energy transition pathways: application to Belgium, Ph.D. thesis, Université Catholique de Louvain, 2021.

[72] G. Limpens, EnergyScope TD documentation, Accessed 2023. URL: https://energyscope.readthedocs.io/en/v2.2/.

[73] IPCC, Climate Change 2013 - The Physical Science Basis, 2014. URL: https://www.ipcc.ch/report/ar5/wg1/.

Chapter 2

EnergyScope Pathway: Its choice and its formulation

2.1 EnergyScope Pathway: The right model

"*Only when single-model results are contextualized by the model's position in the larger ensemble, the reader would be able to have a complete and correct interpretation of the output*" [10]. Energy system models of varying complexity are valuable tools for guiding policymakers and projecting future trends. These models enable the exploration of different energy scenarios and the assessment of their consequences. Specifically, techno-economic models play a crucial role in identifying technically feasible pathways for the energy transition while considering the associated economic costs. These models can be classified based on two key factors: technical resolution and simulation horizon, as illustrated in Figure 2.1.

Increasing the technical resolution of energy system models often comes at the expense of a shorter simulation horizon, and vice versa. For instance, day-ahead grid operation models prioritise accurate grid resolution and capacity reserves in case of foreseeable deviations, but they may not incorporate long-term market trends. Different model classes cater to various needs, with decreasing technical resolution. These include machine-level control, network dispatch, unit commitment, maintenance, power plant expansion, planning for new infrastructure, and scenario analysis. Each class serves a specific purpose, from fine-grained control within a machine to the exploration of multiple assumptions across different scenarios.

In accordance with the previous classification, models aimed at aiding decision-makers in the energy transition primarily fall under the categories of planning and sce-

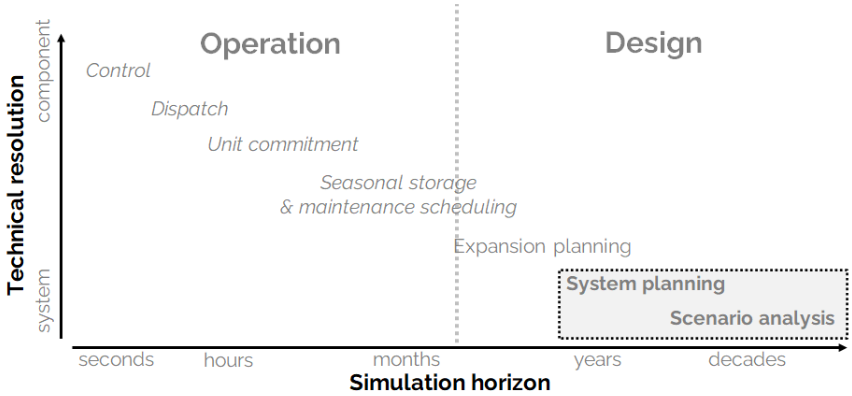

Figure 2.1. Model can be classified by their core focus: **Operation** or **Design**. These categories can be broken down into subcategories. This work focuses on the system planning and scenario analysis models. Inspired from [11].

nario analysis, with a lower technical resolution than the other classes of model (see Figure 2.1). Nonetheless, ensuring technical accuracy is of paramount importance to ensure the effective performance of future energy systems. Hence, these models should meet the following requirements as a minimum: (i) assessment of intermittent renewable energy integration thanks to an **hourly resolution** spanning a one-year time horizon; (ii) accounting for the **whole-energy system** by including all energy (i.e. heat, electricity and mobility) and non-energy flows in different sectors, accounting for their respective greenhouse gas emissions, as well as all resources, conversion processes, and storage technologies; (iii) exploration of all available options through the **optimisation of investments and operations**; (iv) consideration of long-term investments throughout the **transition pathway** process (i.e. 30 years up to 2050, in our case); and (v) ensuring a reasonable **computational time** (i.e. less than one hour on a personal laptop) for analysing different trajectories. Additionally, to enhance result reproducibility and user understanding, it is advantageous for such models to: (vi) maintain transparency and preferably be **open-source**, with accessible data and accompanied by collaborative documentation.

These requirements are commonly found in reviews on energy system models. In 2010, Connolly et al. [12] reviewed 68 tools, considering similar criteria (i.e. (i-iv) and (vi)), along with others such as the “popularity” of the models via the number of downloads/sales or the integration of economic market equilibrium. Eight years later, Lopion et al. [13] enriched the review of Connolly et al. [12] using similar critieria and including models developed in the 2010s. In 2014, Pfenninger et al. [14] pointed out the current paradigms and challenges to face as well as the emerging approaches to address them in the 21st century energy systems modeling community. Besides the behavioral and social factors, they also highlighted the challenges related to mutli-sectorial systems, time and space resolution or the open-accessibility of data and models and their ability to account for uncertainties. In 2019, Prina et al. [15] reviewed 12 "*most established*" models, focusing on criteria (i-ii) and (iv). This review was followed by a classification where criteria (i-iv) were taken into account [16]. In 2021, Chang et al. [17] conducted a survey-based review of 42 models for energy transition modelling, covering all criteria except computational time. Based on these reviews, models are compared based on all the previous criteria except the computational time (v) (see Table 2.1). Indeed, the latter is hard to compare as models are not applied to the same case study and the information is rarely given. The table includes only the models that achieved partially at least four out of the five criteria. We endeavored to update the model's information by consulting the model's website and repository, yet there is a possibility that some information might have been overlooked or omitted inadvertently.

From Table 2.1, four models almost check all the boxes (partially the pathway one): Calliope, GENeSYS-MOD, PyPSA and TIMES.

Calliope

Calliope is a "*tool that makes it easy to build energy system models*" at different geographical scale. Even if the framework offers the possibility of modelling multi-year systems, we did not find a relevant publication on this topic. In fact, the model is typically employed for snapshot analysis, i.e. optimization of a target future year. Previous studies have used the model to investigate the phasing out of fossil and nuclear energies in a multi-regional UK power system [46]. More recently, the model has been applied to analyse a scenario of a multi-energy district in Switzerland [47]. Moreover, the model has been used with decades of weather data. However, its application has been limited to assessing the impact of inter-year variability in wind and PV on the results, rather than evaluating a transition pathway [48].

GENeSYS-MOD

Similarly GENeSYS-MOD presents some limitations. This model is an application of the open-source energy modelling system (OSeMOSYS), itself represented as a model with a poor time discretisation and a heavy computational burden according to

Table 2.1. Comparison of existing models that partially satisfy at least four of the five criteria (in alphabetical order). Legend: ✓criterion satisfied; ✓ criterion partially satisfied; ✗ criterion not satisfied. Data from [12, 15–17]

Model	Ref.	Hourly	Whole-energy	Optimis. invest. & operation	Pathway	Open-source
Calliope	[18, 19]	✓	✓	✓	✗[a]	✓
COMPOSE	[20]	✓	✓	✓	✓	✓[b]
DER-CAM	[21, 22]	✓	✓[c,d]	✓	✗[e]	✓[f]
DIETER	[23]	✓	✓[d,g]	✓	✗[e]	✓
E2M2	[24]	✓	✓[c,d,h]	✓	✓	✗[i]
EMPIRE	[25]	✓	✗[c,d,g,h]	✓	✓	✓[b]
Ener. Trans. Model	[26]	✓	✓	✗[j]	✓	✓
EnergyPLAN	[27]	✓	✓	✗[k]	✗[l]	✓[f]
energyRt	[28]	✓	✓	✓[m]	✓	✓
EnergyScope TD	[29]	✓	✓	✓	✗[l]	✓
Enertile	[30]	✓	✓[d]	✓	✓	✗[n]
ESO-XEL	[31]	✓	✗[c,d,g,h]	✓	✓	✓
GENeSYS-MOD	[32]	✓	✓	✓	✓	✓
H2RES	[33]	✓	✗	✓??	✓	✓
iHOGA	[34]	✓	✗[c,d,g,h]	✓[m]	✓	✓[b]
IMAKUS	[35]	✓	✓[c,d]	✓	✓	✗[i]
OpenDSS	[36]	✓	✓	✗[k]	✓	✓
Plexos	[37]	✓	✓[o]	✓	✓	✗[i]
PyPSA	[39, 40]	✓	✓	✓	✓[p]	✓
RamsesR	[42]	✓	✓[c,d,h]	✓	✓	✓
ReEDS	[43]	✗[q]	✓[d,g,h]	✓	✓	✓[b]
TIMES	[44]	✓	✓	✓	✓	✓[r]

[a] Topic is being discussed in the chat of their repository but not yet included in their documentation.
[b] '*Free under some special conditions*´.
[c] Transport not accounted for.
[d] Industry not accounted for.
[e] Not specified but time horizon is 1 year.
[f] Freeware.
[g] DHN not accounted for.
[h] Individual heating not accounted for.
[i] Commercially (paid) licensed.
[j] The ETM is a simulation model with a simple merit order 'optimisation' for electricity, flexibility and heat.
[k] Simulation model.
[l] Yearly horizon without pathway.
[m] EnergyRT optimises investments only.
[n] Only for internal use.
[o] Does not account for all sectors but allow to implement them according to Waucquez [38].
[p] Pedersen et al. [41] applied PyPSA to a whole energy system split in 37 nodes. Using a myopic approach, the model optimises the energy transition with a 3-hours resolution).
[q] Seasonal time slice.
[r] Model is now open-source with limited access to data [45].

[15]. Löffler et al. [32] applied the model to the world by splitting it into 10 regions and most of the energy demand sectors, leaving to the user the choice of the time resolution. For their application they used representative years with three days and two time slice per day.

PyPSA

Among the open-source models with an active community, PyPSA is one of the best-performing, with a large and active community, development at the state of the art, worldwide applications, and usage not only limited to academia. A study conducted by Bartholdsen et al. [49] centered on Germany employed a representation comprising 16 time slices per representative year. This choice was substantiated by the work of Welsch et al. [50], which demonstrated that this level of temporal granularity yields consistent results in comparison to hourly time resolution over a year. However, it is noteworthy that the utilization of a limited number of time slices may oversimplify the optimization of storage technologies, especially those designed for inter-month energy storage. This simplification can be viewed as a pragmatic approach to reduce the computational burden while over-simplifying the challenge of accurately integrating intermittent renewable energy sources. Furthermore, PyPSA, a modeling framework recognized for its robustness and active user community, has also been employed to investigate scenarios related to myopic transitions [41].

TIMES

The TIMES model, short for The Integrated MARKAL-EFOM System, is a well-established framework renowned for its capacity to generate comprehensive energy models. It encompasses a rich array of features, including support for multi-cell modeling, pathway analysis, full-scale representation of energy systems, and the consideration of market equilibrium dynamics, all of which facilitate thorough scenario exploration. This model has a widespread adoption and has been utilized by worldwide institutions such as the International Energy Agency (IEA) or technical ones such as VITO (Vlaamse Instelling voor Technologisch Onderzoek) research institute. Notably, TIMES was reported as commercial (i.e. not free to download) in 2010 [12]. A more recent survey conducted in 2020-2021 confirmed that the model was using a commercial interface [17]. Recent developments by the IEA-ETSAP have resulted in a version that is compatible with the open-source solver CBC. In various studies conducted in different regions, including Canada, Sweden, the EU, and Denmark, TIMES has been shown to utilize 12 to 32 time-slices annually [16].

To highlight the sensitivity of results to time resolution, Haydt et al. [51] conducted a study focusing on the electrical sector, using up to 12 typical days with an hourly resolution. Regarding data accessibility, while some publications partially present the used dataset, the overall accessibility of TIMES data is not ensured [45].

While Calliope, OSeMOSYS, PyPSA and TIMES frameworks have the potential to be used for evaluating a transition pathway, we have not come across any publication that explicitly demonstrates their application to such cases with an hourly time resolution over significant time slices to accurately capture the seasonality within each representative year. Hence, it appears that none of the models of Table 2.1 fully meets the five criteria outlined in the table, topped with the additional consideration of acceptable computational time. This observation is consistent with the findings presented by Prina et al. [15] who identified two approaches for optimising the energy transition pathway based on the six criteria. The first approach involves running a snapshot model multiple times using an algorithm that optimises the transition path and validates the operability of the system. The second approach aims to extend a snapshot model to represent the entire transition pathway. However, they excluded this option due to the lack of models that met the requirements of being fast enough and easily adaptable. Therefore, they developed a new model based on the first methodology, named EPLANoptTP. It uses a multi-objective evolutionary algorithm to optimise the EnergyPLAN model [27]. To manage computational time, the number of decision variables is limited to three: PV, wind turbine and battery capacities. Thus, the model does not investigate all the options (i.e. criteria (iii)).

For the aforementioned reasons, the current work opted for EnergyScope Pathway, an extension of the open-source and documented EnergyScope TD model [29] listed in Table 2.1. The latter has a time horizon of one year and does not account for the pathway from an existing energy system to a long-term target. The pathway version extends the time horizon to decades and accounts for the pathway transition from an existing energy system to a long term target. The computational time is kept low (i.e. around 15 minutes on a personal laptop), mostly due to keeping the linear formulation after extending the snapshot model. Limpens et al. [52] provides more detailed insights into the modeling choices made during methodological development. In the spirit of the EnergyScope project, the code is fully open-source (under the License Apache 2.0, see repo [53]) with a collaborative documentation [54]. Compared to existing models, EnergyScope Pathway introduces a rapid computational optimisation tool for exploring diverse transition pathways within an entire energy system while maintaining high temporal precision to accurately capture the integration of intermittent renewables.

To the best of our knowledge, there are potentially other frameworks that could be extended to similar capabilities, but their computational times for similar case studies have not been found.

2.2 EnergyScope Pathway and its linear formulation

EnergyScope Pathway is the extension of EnergyScope TD [29] that follows the snapshot approach [55]. The objective of this section is to present the fundamental variables and constraints of the latter based on which the former was developed. Formulation choices have been made but they are not discussed here. The interested reader is invited to refer to Appendix B of [52] for further information in this regard.

2.2.1 The starting point: a scenario analysis model

Typical days to break the curse of dimensionality

In the field of bottom-up energy system modelling[1], one of the biggest challenges is the time resolution [16]. With the rise of VRES, being able to integrate them and capture their interactions with the rest of the energy system requires an hourly time resolution while optimising a whole year (i.e. 8760 hours), if not a whole transition (i.e. several decades). This long-term target combined with a fine time resolution usually leads to the so-called "curse of dimensionality" [56]. As an example, running EnergyScope TD over each of the 8760 hours to optimise a single target year takes more than 19h [29].

To break this curse, EnergyScope TD, like other models [57–59], relies on a subset of representative days called typical days (TDs). This more limited number of days, i.e. 12 in the rest of this thesis, clusters the days of the year that have similar time series of demands (i.e. varying electricity and heat demands) and weather data (i.e. sun, onshore and offshore wind). This way, each day of the year is associated to one of these typical days (see Figure 2.2).

Finally, to properly capture the inter days dynamics, EnergyScope TD uses the "Coupling typical days" method from Gabrielli et al. [57]. Among others, this allows representing the dynamics and the seasonality of storage capacities. This method as well as the clustering approach selected in our case, i.e. k-medoids [60, 61], are

[1] As detailed by Prina et al. [16], bottom-up models offer a detailed analysis of components and interconnections within different energy sectors, allowing for a techno-economic comparison of technologies and assessment of alternatives for achieving energy targets and reducing greenhouse gas emissions. On the contrary, top-down modes, mostly used by economists and administrations, integrate a simplified representation of the energy system as interacting with the other macro-economic sectors.

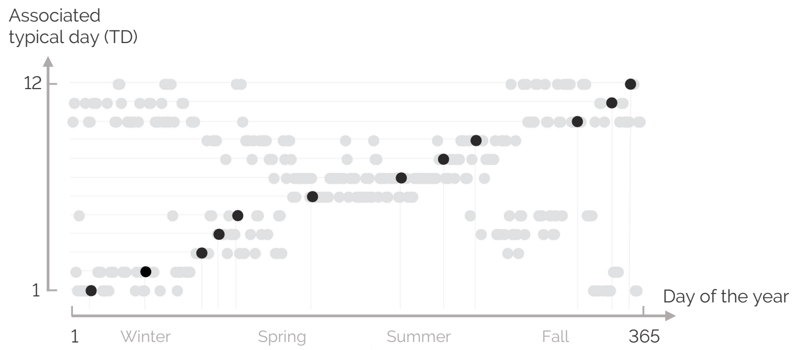

Figure 2.2. Association of each day of the year (gray dots) to one of the 12 typical days (TDs) (black dots). Graph adapted from Limpens et al. [29].

extensively detailed and compared to other methods, in the work of Limpens et al. [29].

Overview of the snapshot model

EnergyScope TD [29] is a model that optimises both the investment and operating strategy of a '*whole*'-energy system, encompassing electricity, heating, mobility, and non-energy sectors. According to Contino et al. [62], a model qualifies as a 'whole-energy' system when it considers all energy sectors, including the non-energy demand such as the production of plastics and other materials using feedstocks that are also considered as energy carriers, with the same level of detail.

The model's hourly resolution over a year makes it well-suited for integrating intermittent renewables. Its formulation incorporates a reconstruction method that captures different time scales from the hour to the season while accounting for the inter-weeks patterns of wind. The model optimises the investment decisions and hourly operations over a year, with a computational time of less than a minute on a personal laptop. This characteristic was intentionally incorporated into the model design to facilitate uncertainty quantification and other studies that require numerous iterations [63].

EnergyScope TD has been successfully applied to various national energy systems, including Switzerland [29, 64], Belgium [65], Italy [66], and other European countries [67]. Furthermore, it has been extended to a multi-region energy system model [68], coupled with other energy models [69], or employed to focus on specific sectors such as the networks of electricity, gas, and hydrogen [70].

Formulation of the snapshot model

The conceptual structure of the model is illustrated in Figure 2.3: given the end-use energy demand, the efficiency and cost of energy conversion technologies, the availability and cost of energy resources, the model identifies the optimal investment and hourly operation strategies to meet the demand and minimise the total annual cost and greenhouse gas emissions of the energy system. Typically, the two objectives are integrated by placing a limit on emissions while simultaneously minimizing the costs.

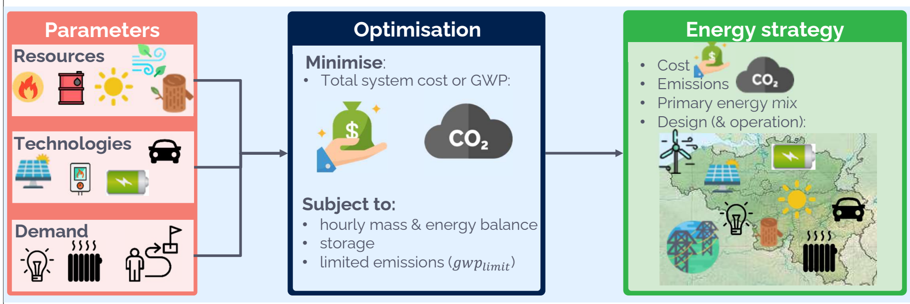

Figure 2.3. EnergyScope TD model is a flow model with inputs (Parameters), an optimizing model (Optimisation) and results (Energy strategy).

Linear formulation

The following section illustrates the formulation of the original EnergyScope TD model. The objective function, cost and greenhouse gases (GHG) formulation are detailed. The rest of the formulation is detailed and available in a previous work [71]. This work uses the following nomenclature: SETs are in capital letters, **Variables** are in bold and with the first letter in upper case, and *parameters* are in italic.

$$\min \ \mathbf{C_{tot}} = \sum_{j \in TECH} \Big(\tau(j) \mathbf{C_{inv}}(j) + \mathbf{C_{maint}}(j) \Big) + \sum_{i \in RES} \mathbf{C_{op}}(i) \tag{2.1}$$

$$\text{s.t. } \tau(j) = \frac{i_{rate}(i_{rate}+1)^{lifetime(j)}}{\Big((i_{rate}+1)^{lifetime(j)} \Big) - 1} \qquad \forall j \in TECH \tag{2.2}$$

The objective, Eq. (2.1), is the minimisation of the total annual cost of the energy system ($\mathbf{C_{tot}}$), defined as the sum of the annualised investment cost of the technologies ($\tau \cdot \mathbf{C_{inv}}$), the operating and maintenance costs of the technologies ($\mathbf{C_{maint}}$) and the operating cost of the resources ($\mathbf{C_{op}}$). The annualised factor τ is computed *a priori* based on the interest rate (i_{rate}) and the technology lifetime, (*lifetime*), Eq. (2.2).

$$\mathbf{C_{inv}}(j) = c_{inv}(j)\mathbf{F}(j) \qquad \forall j \in TECH \tag{2.3}$$

$$\mathbf{C_{maint}}(j) = c_{maint}(j)\mathbf{F}(j) \qquad \forall j \in TECH \quad (2.4)$$

The total investment cost ($\mathbf{C_{inv}}$) of each technology results from the multiplication of its specific investment cost (c_{inv}) and its installed capacity ($\mathbf{F}$), see Eq. (2.3). The installed capacity is defined with respect to the main end-uses output type, such as electricity for PV or heat for a boiler. The total operation and maintenance costs ($\mathbf{C_{maint}}$) are calculated in the same way, Eq. (2.4).

$$\mathbf{C_{op}}(i) = \sum_{t \in T} c_{op}(i)\mathbf{F_t}(i,t)t_{op}(t) \qquad \forall i \in RES \quad (2.5)$$

The total cost of the resources ($\mathbf{C_{op}}$) is calculated as the sum of the end-use over the different time-periods multiplied by the period duration (t_{op}) and the specific cost of the resources (c_{op}), Eq. (2.5). To simplify the reading, we write the sum over typical days as $t \in T$ such as in Eq. (2.5). The period T represents the sequence of hours and typical days over a year (8760h)[2]. The full formulation is detailed in [29] or in the documentation [72].

$$\mathbf{GWP_{tot}} = \sum_{i \in RES} \mathbf{GWP_{op}}(i) \quad (2.6)$$

$$\mathbf{GWP_{op}}(i) = \sum_{t \in T} gwp_{op}(i)\mathbf{F_t}(i,t)t_{op}(t) \qquad \forall i \in RES \quad (2.7)$$

The global annual GHG emissions are calculated using a life cycle assessment (LCA) approach, i.e. taking into account emissions of the resources '*from cradle to use*'. It is based on the indicator '*GWP100a-IPCC2013´* developed by the intergovernmental panel on climate change (IPCC) [73]. For climate change, the natural choice as indicator is the global warming potential, expressed in ktCO_2-eq./year. In Eq. (2.6), the total yearly emissions of the system ($\mathbf{GWP_{tot}}$) are defined as the emissions related to resources ($\mathbf{GWP_{op}}$). The total emissions of the resources are the emissions associated to fuels (from cradle to combustion) and imports of electricity (gwp_{op}) multiplied by the period duration (t_{op}), Eq. (2.7). Thus, this version accounts only for operation without accounting for the global warming potential (GWP) emitted during the construction of the technologies. This makes the results comparable with metrics used in the reports by the European Commission and the International Energy Agency (IEA).

The above equations (Eqs. (2.1) - (2.7)) represent only a part of the formulation and illustrate the syntax that is used. Those representing the energy balance, network implementation, sectors representation, etc. are not presented in this work but are detailed in the latest version of the model, see [71] and in the documentation [72].

[2]The exception is storage level which is optimised over the 365 days of the year instead of typical days.

Finally, energy storage has two dimensions to be optimised: (i) the hourly power flow, encompassing both charging and discharging and, (ii) the stored energy quantity (also referred to as 'storage level'). EnergyScope TD optimises the former based on the hourly resolution of the typical days and the latter over the entire span of 8760 hours in a year. This formulation allows for the effective integration of a wide range of energy storage technologies, spanning short-term solutions like small thermal storage units and daily-use batteries, to longer-term options such as hydro-dam storage for seasonal storage, and even large-scale thermal storage for intra-week patterns. A previous study investigated the roles of various storage technologies, considering their sectoral applications and temporal aspects, within the context of the Swiss energy system [64].

2.2.2 Extending the model for pathway optimisation

In this section, we delve into the extension of EnergyScope TD from a static yearly snapshot model to a comprehensive pathway model. While snapshot models provide insights into the energy system for individual years, they lack the capacity to capture the dynamics inherent in investment strategies throughout a transition period. The proposed approach involves segmenting the transition into five-year intervals. This approach results in seven instances of EnergyScope TD – called representative years – spanning the 30-year transition period, covering the years from 2020 to 2050. To bridge these representative years, we introduce additional constraints that capture the investments changes between consecutive periods, accounting for societal inertia and evaluating both the cost implications and emissions of the transition (see Figure 2.4). Overall, these constraints are integrated into a linear framework, ensuring computational efficiency, with an approximate computational time of 14 minutes on a personal laptop (2.4 GHz Intel Core i5 quad-core). Simplification and choices were necessary to implement linearly the problem while keeping a tractable computational time. In this section, the retained formulation is presented.

The proposed formulation relies on representative years, selected every 5 years from 2020 to 2050. The period between two of them is called '*PHASE*´. For each of these 7 representative years, the EnergyScope TD model is run using the relevant data (such as energy demand, technology costs or GHG emissions constraints).

As a consequence, a new dimension '*year*' is added to all **Variables** and parameters, except the interest rate (i_{rate}) assumed constant during the transition. This new dimension is necessary to represent the changes of technology and resource characteristics over the representative years. As an example, the investment cost (c_{inv}) of solar photovoltaic panels could drastically vary in the next decades (e.g. data used

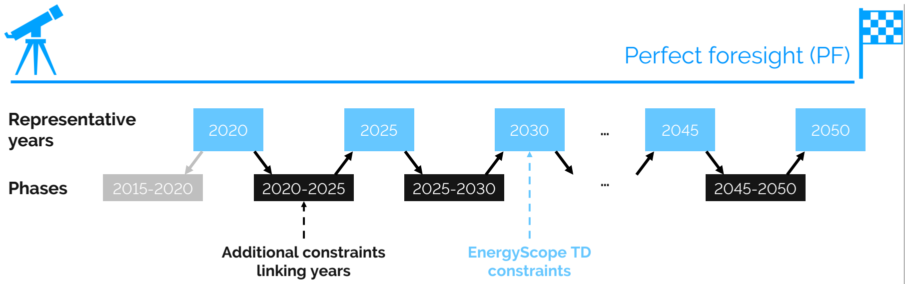

Figure 2.4. The pathway methodology relies on 7 representative years (blue boxes) where the model EnergyScope Typical Days (EnergyScope TD) is applied. Moreover, the formulation accounts for linking constraints (black boxes) and an initial condition (grey box). The overall problem is the pathway model.

ranges between 1220 to 870 [$€_{2015}$/kW] between 2020 and 2035).

Linking years

At this stage, all years are independent. In the following, we introduce new constraints to link representative years. The formulation allows to install new capacity ($\mathbf{F_{new}}$), remove a capacity that has reached its lifespan ($\mathbf{F_{old}}$) or decommission a technology prematurely ($\mathbf{F_{decom}}$). These capacity changes occur during a phase, this implies that there is no capacity change during a representative year. Figure 2.5 illustrates the concept.

$$\mathbf{F}(y_{\text{stop}}, i) = \mathbf{F}(y_{\text{start}}, i) + \mathbf{F_{new}}(p, i) - \mathbf{F_{old}}(p, i) - \sum_{p2 \in PHASE \cup \{2015\_2020\}} \mathbf{F_{decom}}(p, p2, i)$$

$$\forall p \in PHASE, y_{stop} \in Y\_STOP(p), y_{start} \in Y\_START(p), i \in TECH \quad (2.8)$$

Similarly to a mass balance, Eq. (2.8) is the technology capacity balance. The constraint forces the installation or withdrawing of capacities between two representative years: at the end of the phase (y_{stop}), the available capacity is the one used in the next representative year ($\mathbf{F}(y_{stop})$). This capacity is equal to the one available in the previous representative year ($\mathbf{F}(y_{start})$) plus the new installed capacity ($\mathbf{F_{new}}$) minus the capacity that has reached its lifetime ($\mathbf{F_{old}}$) minus the early decommissioned capacity ($\mathbf{F_{decom}}$). One notices that the capacity available for each representative year depends on a year (y_{start} or y_{stop}), while the other capacity changes depend on a phase (p or $p2$). Moreover, the decommissioning term depends on another phase, which is the one when the technology decommissioned has been built. As an illustration, Figure 2.5

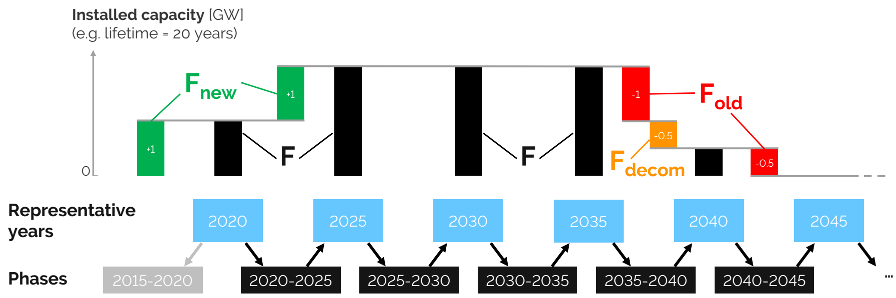

Figure 2.5. Example of how the technology capacities and associated variables are evolving. The example uses a technology with a 20 years lifetime. Initially 1 GW of capacity exists ($\mathbf{F_{new}}$ during phase 2015_2020). Then another 1 GW is deployed ($\mathbf{F_{new}}$ during phase 2020_2025). 15 years later, a part of the capacity reaches its lifetime limit and is removed ($\mathbf{F_{old}}$ phase 2035_2040). Moreover, during the latter phase, additional capacity is decommissioned prematurely ($\mathbf{F_{decom}}$). Finally, the technology reaches its expected lifetime and is fully withdrawn ($\mathbf{F_{old}}$).

gives an example where 0.5 GW of a capacity built in 2015_2020 is decommissioned in 2030_2035 ($\mathbf{F_{decom}}$(2030_2035,2015_2020,i)).

$$\mathbf{F_{decom}}(p, p2, i) = 0$$
$$\forall i \in TECH, p \in PHASE, p2 \in PHASE \cup \{2015\_2020\} | decom_{allowed}(p, p2) = 0 \quad (2.9)$$

$$\mathbf{F_{old}}(p, i) = \quad \text{if}(age = \text{‘}STILL\_IN\_USE\text{’}) \text{ then} 0$$
$$\text{else} \left(\mathbf{F_{new}}(age, i) - \sum_{p2 \in PHASE} \mathbf{F_{decom}}(p2, age, i) \right)$$
$$\forall p \in PHASE, \forall j \in TECH | age \in AGE(p, j) \quad (2.10)$$

In linear programming, a solution might be mathematically correct, while not making sense in practice. As an example, a technology could be decommissioned before being built ($p < p_{built}$). Eqs. (2.9-2.10) allow preventing these non-sense while keeping the formulation linear. Eq. (2.9) forces the decommissioned capacity to zero when technology will be built after. To do so, a parameter ($decom_{allowed}$) is defined *a priori* and is equal to 0 or 1 when decommissioning is not possible or possible, respectively. Eq. (2.10) defines the capacity reaching its lifetime limit at a certain phase, the concept is illustrated in Figure 2.5. For each phase, a set (AGE) is calculated *a priori*. It relates, for a given phase and technology, when the technology was built. In the case the technology has already reached its lifetime limit, the set (*AGE*) returns the phase when the technology has been built. The first part of Eq. (2.10) indicates that the technology is still available, and thus no capacity needs to be removed. The second part of the equation represents the capacity that reached its expected lifetime minus a part of the capacity that would have been decommissioned. As an example, Figure 2.5 shows a 20 years lifetime technology with 1 GW of capacity installed before 2020. The 'if' in Eq. (2.10) is linear as it is applied to a parameter and not a variable.

$$\mathbf{F_{new}}(\mathit{2015\_2020}, i) = \mathbf{F}(\mathit{YEAR\_2020}, i) \qquad \forall i \in \mathit{TECH} \quad (2.11)$$

To initialise the problem in 2020 with the existing design, an additional phase '*2015_2020*' is created. Eq. (2.11) requires that the capacity used in 2020 is installed in the previous phase.

Society inertia

To avoid unrealistically fast changes in the system, additional constraints are needed during the phases for the mobility and low temperature heat sectors. Without the following constraints, the model would eliminate certain technologies in one phase, such as oil and gas decentralised boilers. Even if this result is mathematically and physically correct, (i.e. fuels are expensive and investing in more efficient technology is economically and environmentally more profitable), this swap of technology cannot occur in one phase (i.e. 5 years). Indeed, society inertia to change, available manpower, supply chains and manufacturers limit the change.

$$\mathbf{\Delta_{change}}(p, i) \geq \sum_{t \in T} \big(\mathbf{F_t}(y_{start}, i, t)\big) - \sum_{t \in T} \big(\mathbf{F_t}(y_{stop}, i, t)\big)$$
$$\forall j \in \mathit{TECH}, p \in \mathit{PHASE}, y_{start} \in \mathit{Y\_START}(p), y_{stop} \in \mathit{Y\_STOP}(p) \quad (2.12)$$

$$\sum_{i \in TECH(HeatLowT)} \mathbf{\Delta_{change}}(p, i) \leq lim_{LT,ren} \cdot \big(eui(y_{start}, HotWater) + eui(y_{start}, SpaceHeat)\big)$$
$$\forall p \in \mathit{PHASE}, y_{start} \in \mathit{Y\_START}(p) \qquad (2.13)$$

$$\sum_{i \in TECH(MobPass)} \mathbf{\Delta_{change}}(p, i) \leq lim_{MobPass} \cdot eui(y_{start}, MobPass))$$
$$\forall p \in \mathit{PHASE}, y_{start} \in \mathit{Y\_START}(p) \qquad (2.14)$$

$$\sum_{i \in TECH(MobFreight)} \mathbf{\Delta_{change}}(p, i) \leq lim_{MobFreight} \cdot eui(y_{start}, MobFreight)$$
$$\forall p \in \mathit{PHASE}, y_{start} \in \mathit{Y\_START}(p) \qquad (2.15)$$

Eq. (2.12) calculates the upper limit of change ($\Delta_{\mathbf{change}}$) in terms of supplied demand instead of installed capacity. Based on this quantification, the amount of change per phase is limited for low temperature heat ($lim_{LT,ren}$), Eq. (2.13), passenger mobility ($lim_{MobPass}$), Eq. (2.14) and freight mobility ($lim_{MobFreight}$), Eq. (2.15). For instance, if the maximum allowable variation in supplied low temperature heat is set at 25%, it would restrict the technology-related changes in low temperature heat to 25% within a given phase. Consequently, if a technology supplies more than 25% of the low temperature heat, it would require multiple phases to replace it with a different technology.

Cost and emissions of the transition

To optimise the energy system, two key metrics must be adapted: the transition cost and the total global warming potential (GWP). Concerning the first one, all costs are expressed in €$_{2015}$ and an annualisation factor is used to distinguish investments over the transition. For the GWP, the metric used is based on the contributions of the gases over 100 years. It is assumed that the impact of emitting at the beginning or the end of transition are equivalent and thus no annualisation is used.

$$\min\ \mathbf{C_{tot,trans}} = \mathbf{C_{tot,capex}} + \mathbf{C_{tot,opex}} \tag{2.16}$$

$$\mathbf{C_{tot,capex}} = \sum_{p \in PHASE \cup \{2015\_2020\}} \mathbf{C_{inv,phase}}(p) - \sum_{i \in TECH} \mathbf{C_{inv,return}}(i) \tag{2.17}$$

$$\mathbf{C_{tot,opex}} = \mathbf{C_{opex}}(2020) + t_{phase} \cdot \tau_{phase}(p) \cdot \sum_{p \in PHASE | y_{\text{start}} \in P\_START(p), y_{\text{stop}} \in P\_STOP(p)} \Big(\mathbf{C_{opex}}(y_{\text{start}}) + \mathbf{C_{opex}}(y_{\text{stop}}) \Big) / 2 \tag{2.18}$$

$$\tau_{phase}(p) = 1/(1 + i_{rate})^{diff\_2015\_year(p)} \tag{2.19}$$

As an extension of Eq. 2.1, the objective function to be minimised is the total transition cost of the energy system ($\mathbf{C_{tot,trans}}$), defined as the sum of the total capital expenditure (CAPEX) ($\mathbf{C_{tot,capex}}$) and the operational expenditure (OPEX) ($\mathbf{C_{tot,opex}}$), according to Eq. (2.16). The total CAPEX ($\mathbf{C_{tot,capex}}$) is the sum of the investment during each phase ($\mathbf{C_{inv,phase}}$), Eq. (2.17), to which the residual asset value in 2050 is withdrawn ($\mathbf{C_{inv,return}}$). Thus, the investments account for the installation and dismantlement costs of the technologies. The total OPEX ($\mathbf{C_{tot,opex}}$) is the sum of the OPEX in 2020 and the annualised sum of the OPEX during each phase ($\mathbf{C_{opex}}$), Eq. (2.18). During a phase, the system OPEX is the product of the annualised phase factor, defined in Eq. (2.19), and the arithmetic average of OPEX cost for the representative years before and after the phase. The annualised phase factor is defined based on an average interest rate during the transition.

$$\mathbf{C_{opex}}(y) = \sum_{i \in TECH} \mathbf{C_{maint}}(y, i) + \sum_{j \in RES} \mathbf{C_{op}}(y, j) \qquad \forall y \in YEARS \quad (2.20)$$

For each year, the yearly OPEX ($\mathbf{C_{opex}}$) is the sum of the operating and maintenance costs of technologies ($\mathbf{C_{maint}}$) and the operating cost of the resources ($\mathbf{C_{op}}$), Eq. (2.20).

$$\mathbf{C_{inv,phase}}(p) = \sum_{j \in TECH} \mathbf{F_{new}}(p, j) \cdot \tau_{phase}(p) \cdot \left(c_{inv}(y_{start}, j) + c_{inv}(y_{stop}, j)\right) /2$$
$$\forall p \in PHASE | y_{\text{start}} \in P\_START(p), y_{\text{stop}} \in P\_STOP(p) \quad (2.21)$$

The investment during a phase ($\mathbf{C_{inv,phase}}$) results from the multiplication of the newly built technologies ($\mathbf{F_{new}}$) with their annualised arithmetic averaged specific cost, Eq. (2.21). The annualised phase factor (defined by Eq. (2.19)) is used. The specific cost during the phase is defined as the average between the investment cost for the first and last year of the period.

$$\mathbf{C_{inv,return}}(i) = \sum_{p \in PHASE \cup \{2015\_2020\} | y_{\text{start}} \in Y\_START(p), y_{\text{stop}} \in Y\_STOP(p)} \tau_{phase}(p) \cdot \left(c_{inv}(y_{start}, i) + c_{inv}(y_{stop}, i)\right) /2 \cdot$$
$$\frac{remaining\_years(i, p)}{lifetime(y_{\text{start}}, i)} \left(\mathbf{F_{new}}(p, i) - \sum_{p2 \in PHASE} \mathbf{F_{decom}}(p2, p, i) \right) \quad \forall i \in TECH \quad (2.22)$$

A part of the investment will remain after 2050. This residual investment, also called salvage value, can be calculated for each technology. A parameter, calculated *a priori* , gives for each technology and construction phase, the remaining amount of years (*remaining_years*). As an example, if a PV panel has been built in 2045 and has a 20 years lifetime, the parameter will equal to 15 years. Thus, the salvage value is a fraction of the investment cost of this technology when it has been built. This fraction is the ratio between the number of remaining years and the lifetime of the technology. In the previous example, the residual investment of the PV built is 75%. Eq. (2.22) computes, for each technology, the residual value that must be subtracted from the total cost. The residual value reflects the fact that the technology can still be used after the horizon of the model and is not fully amortised. The residual value is not applied to technologies that are removed prematurely. This differ from other models, such as Plexos where a technology removed prematurely will benefit from its salvage value (see analysis of [38]).

$$\mathbf{GWP_{tot,trans}} = \mathbf{GWP_{tot}}(2020) + t_{phase} \sum_{p \in PHASE | y_{\text{start}} \in Y\_START(p), y_{\text{stop}} \in Y\_STOP(p)} /2 \left(\mathbf{GWP_{tot}}(y_{\text{start}}) + \mathbf{GWP_{tot}}(y_{\text{stop}}) \right) \tag{2.23}$$

$$\mathbf{GWP_{tot,trans}} \leq gwp_{lim,trans} \tag{2.24}$$

The total global warming potential (GWP) emissions during the transition ($\mathbf{GWP_{tot,trans}}$) are equal to the sum of the total emissions per period ($\mathbf{GWP_{tot}}$), Eq. (2.23). The emissions during a phase is estimated as the arithmetic average of the representative years before and after the phase. Eq. (2.24) limits the total GWP emissions during the transition by a maximum ($gwp_{lim,trans}$).